Structure and Function of the Middle Domain of ClpB from Escherichia coli

ARTICLE *in* BIOCHEMISTRY · JANUARY 2004

Impact Factor: 3.02 · DOI: 10.1021/bi035573d · Source: PubMed

4 AUTHORS, INCLUDING:

Sabina Kedzierska-Mieszkowska
University of Gdansk
32 PUBLICATIONS **417** CITATIONS
SEE PROFILE

Vladimir Akoyev
Ventria Bioscience
31 PUBLICATIONS **271** CITATIONS
SEE PROFILE

Published in final edited form as:
Biochemistry. 2003 December 9; 42(48): 14242–14248.

Structure and Function of the Middle Domain of ClpB from *Escherichia coli*[†]

Sabina Kedzierska[‡], **Vladimir Akoev**[§], **Micheal E. Barnett**[§], and **Michal Zolkiewski**[*,§]
Department of Biochemistry, Kansas State University, Manhattan, Kansas 66506 and Department of Biochemistry, University of Gdansk, Gdansk, Poland

Abstract

ClpB belongs to the Hsp100/Clp ATPase family. Whereas a homolog of ClpB, ClpA interacts with and stimulates the peptidase ClpP, ClpB does not associate with peptidases and instead cooperates with DnaK/DnaJ/GrpE in an efficient reactivation of severely aggregated proteins. The major difference between ClpA and ClpB is located in the middle sequence region (MD) that is much longer in ClpB than in ClpA and contains several segments of coiled-coil-like heptad repeats. The function of MD is unknown. We purified the isolated MD fragment of ClpB from *Escherichia coli* (residues 410–570). Circular dichroism (CD) detected a high population of α -helical structure in MD. Temperature-induced changes in CD showed that MD is a thermodynamically stable folding domain. Sedimentation equilibrium showed that MD is monomeric in solution. We produced four truncated variants of ClpB with deletions of the following heptad-repeat containing regions in MD: (417–455), (456–498), (496–530), and (531–569). We found that the removal of each heptad-repeat region within MD strongly inhibited the oligomerization of ClpB, which produced low ATPase activity of the truncated ClpB variants as well as their low chaperone activity *in vivo*. Only one ClpB variant (Δ417–455) could partially complement the growth defect of the *clpB*-null *E. coli* strain at 50 °C. Our results show that heptad repeats in MD play an important role in stabilization of the active oligomeric form of ClpB. The heptad repeats are likely involved in stabilization of an intra-MD helical bundle rather than an inter-subunit coiled-coil.

ClpB belongs to the Hsp100 family of proteins, also known as Clp ATPases (1), a class within the AAA^+ superfamily of ATPases associated with various cellular activities (2;3). A unifying structural property of AAA^+ ATPases is the formation of single oligomeric rings with a 6-fold or 7-fold symmetry. Among Clp ATPases, bacterial proteins ClpA, ClpX, and ClpY (HslU) unfold protein substrates and deliver them to the associated peptidases for degradation (4–6). The mechanism of this activity involves an ATP-dependent threading of a protein substrate through a channel within the oligomeric ring of a Clp protein. In contrast, bacterial ClpB (7–9), yeast Hsp104 (10), and plant Hsp101 (11) belong to multi-chaperone systems (with Hsp70 and Hsp40) that reactivate strongly aggregated proteins and do not apparently participate in protein degradation. The mechanism of ClpB-assisted protein disaggregation is currently unknown.

Whereas ClpX and ClpY contain a single ATP-binding AAA domain, two such AAA modules (D1 and D2) are found in ClpA and ClpB (Figure 1A). Each AAA module contains a number of conserved amino-acid sequence motifs, including Walker A and B nucleotide-binding

[†]This work was supported by the National Institutes of Health grant GM58626 and the Kansas Agricultural Experiment Station (contribution 04-070-J).

* To whom correspondence should be addressed: Department of Biochemistry, Kansas State University, 104 Willard Hall, Manhattan, KS 66506. Phone: (785) 532-3083. Fax: (785) 532-7278. E-mail: michalz@ksu.edu..
[‡]University of Gdansk
[§]Kansas State University

motifs. AAA modules also contain sequence motifs that stabilize the oligomeric structure of Clp ATPases (12;13). In addition to ATP-binding modules, Clp ATPases contain less-conserved N-terminal domains that may be involved in substrate recognition and/or processing (14–17).

The two AAA modules in ClpB are separated by a ~160-residue-long sequence region that is not found in ClpA (1). The presence of this "linker" or "middle domain" (MD1, see Figure 1A) is the most conspicuous difference between the sequences of ClpB, a protein-disaggregating chaperone, and ClpA, a protein unfolding component of a protease. The middle domain is essential for the chaperone activity of ClpB (17). This result is consistent with an earlier report that ClpB, but not ClpA, is essential for protein folding *in vivo* under stress conditions (18). Biochemical properties of the middle domain of ClpB and the linkages between the sequence motifs within MD and the activity of ClpB have not been explored yet.

The sequence of MD in ClpB contains several segments of periodic seven-residue repeats, in which the first position (*a*) and the fourth one (*d*) are occupied by predominantly hydrophobic amino acids, whereas the neighboring positions (*g* and *e*, respectively) are often occupied by charged residues (Figure 1B). The characteristic heptad repeats are found in proteins that contain coiled-coils, superhelical complexes of two or more α-helices (19). The coiled-coil structure is stabilized by both hydrophobic (positions *a*, *d*) and electrostatic interactions (positions *e*, *g*). Heptad repeats within the middle domain of ClpB and other related Clp ATPases suggest, therefore, that MDs may have a coiled-coil architecture (20). Coiled-coils, a widely-used protein-protein interaction motif, stabilize the structure of many oligomeric proteins including transcription factors, fibrous proteins (keratin, myosin, fibrinogen) (19), and viral fusion proteins (21). A possible role of putative coiled-coils within ClpB is unknown.

In this study, we explored the structural and functional role of the middle domain of ClpB. We have produced and characterized the isolated MD. We also focused on four apparent coiled-coil repeats within MD and produced four truncated variants of ClpB, each with a deletion removing one of the four repeat segments (see Figure 1B). Our results show that the integrity of the coiled-coil repeats within MD is essential for the structural stability of ClpB and its biological activity.

EXPERIMENTAL PROCEDURES

DNA constructs

A fragment of the *clpB* gene *c*orresponding to the entire MD (amino acids 410–570) was produced by polymerase chain reaction using TaqPlus Precision PCR System (Stratagene) and pClpB (22) as the template and subsequently subcloned between the *Nde*I and *BamH*I sites of pET-14b vector (Novagen).

For the complementation study (see Figure 4), the entire *clpB* gene together with the σ^{32}-dependent promoter was amplified from pClpB by PCR and then subcloned between the *Xma*I and *Pst*I sites of a low copy plasmid, pGB2 (spc^R, str^R) (23). The resulting *clpB*-containing plasmid (pClpB7) was used to create four truncated derivatives (see Figure 1B). Δ 417–455 and Δ 456–498 variants were generated by a double digestion of pClpB7 with *Pvu*I and *Sca*I or *Sca*I and *Bsm*FI, respectively, blunt-ended with T4 DNA polymerase (Promega) and then re-ligated. The two remaining ClpB variants, Δ496–530 and Δ531–569, were created by PCR. The PCR products were digested with endonucleases and then ligated into the linearized pGB2/*Xma*I-*Pst*I vector. Deletions in *clpB* were confirmed by the DNA sequencing facility at Iowa State University (Ames, IA). DNA primers were synthesized by Integrated DNA Technologies, Inc. (Coralville, IA).

For purification of the truncated ClpB, all *clpB* variants produced in pGB2 were amplified by PCR (without σ^{32} promoter) and subcloned between the *Nde*I and *Xho*I sites of pET-20b vector (Novagen).

In vivo ClpB activity assay - a complementation study

The *Escherichia coli* strain MC4100Δ*clpB*::kan (22) obtained from Dr. C. L. Squires (Tufts University, Boston, MA) was transformed with pGB2, pClpB7, or the recombinant derivatives of pClpB7: pΔ417–455, pΔ456–498, pΔ496–530, pΔ531–569. *E. coli* MC4100 (SG20250) (*ara*D139, Δ (*argF-lac*)*U*169, *rps*L150, *rel*A1, *deo*C1, *pts*F25, *rps*R, *flb*B5301) kindly provided by Dr. S. Gottesman (National Institutes of Health, Bethesda, MD) was used as a wt control. Bacteria were grown in LB medium supplemented with spectinomycin (50 μg/mL) to A_{600}=0.3–0.4 and then were transferred to a 50 °C-water bath for 60, 120 and 180 min. Before the temperature shift to 50 °C and at each selected time, 100-μ l culture aliquots were withdrawn and serially diluted in 0.9% NaCl from 1:10 to $1:10^6$. Subsequently, 100 μ l from the last four dilutions were spotted on LB agar plates, which were then incubated for 16–20 h at 37 °C. Cell survival was determined as the number of bacterial colonies multiplied by the appropriate dilution factor. Three independent replicas were carried out for this *in vivo* experiment.

Proteins

MD of ClpB was expressed as a His-tag fusion protein in *E. coli* BL21(DE3) cells (Novagen) and purified using the same procedure as that used before to obtain the N-terminal domain of ClpB (24). Wild-type ClpB and its truncated variants were overproduced in *E. coli* BL21(DE3) and purified as described previously (13). After purification, the proteins were extensively dialyzed against an appropriate buffer (see figures). Protein concentrations were determined spectrophotometrically using the absorption coefficients (in a 1-cm cuvette), A_{280}(0.1%) of 0.347 for wt ClpB, 0.352 for Δ417–455, 0.290 for Δ456–498, 0.349 for Δ496–530, 0.302 for Δ531–569, and 0.662 for the isolated MD. The absorption coefficients were determined from the amino-acid composition of the protein variants using ProtParam program (http://www.expasy.org/tools/protparam.html).

For Western Blotting (see Figure 4B), 0.1% SDS-10% PAGE was performed followed by the electrotransfer of proteins onto a nitrocellulose membrane BA85 (Schleicher and Schuell, Germany). ClpB and its variants were detected using rabbit polyclonal anti-ClpB antibodies (24), a peroxidase-coupled goat anti-rabbit secondary antibody (Southern Biotechnology Associates, Inc., Birmingham, AL), and visualized by a chemiluminescence detection method (Pierce).

Circular dichroism spectroscopy

The CD data were obtained with a Jasco J-720 spectropolarimeter for 1 mg/mL protein in 50 mM Tris-HCl (pH 7.5), 10 % glycerol, 1mM EDTA, 20 mM $MgCl_2$ and 0.2 M KCl using 0.02-cm water-jacketed cylindrical cell connected to an external water bath (Fisher Isotemp 1016P). For thermal stability studies of MD, the temperature of the cell was increased step-wise and the sample was equilibrated at a given temperature until a steady CD signal was obtained. The temperature-induced changes in CD were analyzed using a two-state thermodynamic model (25).

Analytical Ultracentrifugation

A Beckman Optima XL-1 analytical ultracentrifuge was used in sedimentation studies. Sedimentation equilibrium of MD was performed using a 6-channel analytical cell at 40,000 rpm at 4 °C. The concentrations of MD were 0.5, 1, and 2 mg/mL in 50 mM Hepes-KOH (pH 7.5), 20 mM $MgCl_2$, and 1mM EDTA. The data were analyzed using a single-species model

with the software supplied with the instrument (Beckman). Sedimentation velocity experiments were performed at 40,000 rpm at 20 °C with a two-channel aluminum cells. The protein concentration was 1.5 mg/mL in 50 mM Hepes-KOH (pH 7.5), 20 mM $MgCl_2$ 1mM EDTA and 2 mM β -mercaptoethanol. The data were analyzed using the time-derivative method (26) with the software distributed with the instrument.

Gel Filtration Chromatography

HPLC gel filtration experiments were performed at room temperature using a Superose 6 PC 3.2/30 column (Amersham Pharmacia Biotech) with a Shimadzu HPLC system containing an LC-10ATvp solvent delivery unit and an SPD-M10Avp photodiode array detector. Aliquots (20 μ l) of the purified ClpB proteins at ~2.5 mg/mL were chromatographed on the column equilibrated with 50 mM Tris-HCl (pH 7.5), 20 mM $MgCl_2$, 0.2 M KCl, 1 mM EDTA, 1 mM DTT in the absence or presence of 2 mM ATP. Gel filtration protein standards were purchased from BioRad.

ATPase activity determination

The rate of ATP hydrolysis by wild-type ClpB and its truncatedvariants (5 μ g/mL) was determined in the absence or presence of 0.1 mg/mL κ -casein (Sigma) or 0.01 mg/mL poly-L-lysine (Sigma) using the EnzChek Phosphate Assay Kit (Molecular Probes, Eugene, OR). 1-mL reaction solutions contained 100 mM Tris-HCl (pH 7.5), 10 mM $MgCl_2$, 5 mM ATP, 1 mM EDTA, 1 mM DTT, 200 mM MESG substrate (2-amino-6-mercapto-7-methyl-purine riboside), and 1 unit of purine nucleoside phosphorylase (PNP). After incubation at 37 °C, the absorbance at 360 nm was measured and corrected for the background signal. The increases of phosphate concentration were linear up to 45 min of the incubation time. All ATPase assays were performed in duplicates.

RESULTS

First, we asked whether the middle sequence region of ClpB forms a stable protein domain. We purified the 160-residue-long middle fragment of ClpB (see Figure 1A) as a His-tag fusion protein (predicted molecular weight, 21.1 kDa). The circular dichroism (CD) spectrum of MD at room temperature (Figure 2A) showed a negative double band with the minima at 208 and 222 nm. The characteristic shape of the CD spectrum indicates that MD folds into a structure that is dominated by α-helices. Furthermore, the structure of MD is thermodynamically stable, as shown by a cooperative unfolding transition (Figure 2B). The thermal unfolding of MD is accompanied by a loss of the α-helical structure because the CD spectrum of MD at 82 °C indicates a high population of the random-coil conformation (see Figure 2A). The thermal unfolding of MD is reversible with >94% of the CD signal recovered after cooling the MD sample back to 25 °C (data not shown). As shown in Figure 2B, the unfolding of MD can be approximated by a two-state model with the mid-point temperature of 52.1 °C and the unfolding enthalpy of 34.2 kcal/mol. We conclude that the middle sequence fragment of ClpB contains a single stable, predominantly α-helical domain. This result is consistent with the prediction of α-helical coiled-coils within MD.

Since coiled-coils often support protein oligomerization, we investigated the self-association properties of MD in solution. A simultaneous analysis of three sedimentation equilibrium data sets for MD in a low-salt buffer (Figure 3) indicates that the solution of MD contains a single ~21-kDa molecular species. A similar molecular weight of MD was measured in sedimentation equilibrium experiments in 0.3 M KCl (not shown). In contrast, the full-length ClpB forms fully-assembled oligomers under low ionic strength conditions (27) and is a mixture of oligomeric species under physiological ionic strength (28). The results of sedimentation

equilibrium show that MD is monomeric in solution and suggest that putative coiled-coils within MD may not be involved in inter-chain interactions.

Next, we investigated the role of the middle domain in the structural integrity and biochemical functionality of ClpB. As it has been shown before, a deletion of the entire MD from ClpB produces a loss of the chaperone activity (17). Here, we focused on the role of the apparent coiled-coil regions in the MD sequence. We produced four truncated variants of ClpB, each with a deletion of a heptad repeat-containing region (see Figure 1B).

The *in vivo* chaperone activity of the truncated ClpB variants was tested in a complementation experiment involving a *clpB*-null strain of *E. coli* (22). Compared to wt *E. coli*, the *clpB*-null strain containing a low-copy pGB2 plasmid poorly survives heat-shock (Figure 4A). Survival of the mutant cells at lethal temperatures can be restored after expression of the full-length ClpB from pGB2, which confirms the essential role of ClpB in bacteria under severe stress conditions. In contrast, expression of the four variants of ClpB with deletions within MD does not restore the viability of cells under heat-shock in spite of similar amounts of all ClpB forms being produced in the cells (see Figure 4B). Among the truncated variants, only Δ417–455 shows a weak protective effect *in vivo* (see Figure 4A). We conclude that deletions of the heptad repeat-containing regions within MD strongly inhibit the chaperone activity of ClpB.

To test whether the loss of the activity *in vivo* may be related to a loss of structural integrity in the truncated ClpB, we purified the four variants of ClpB with deletions within MD and compared their properties to those of the wild type full-length ClpB. Circular dichroism spectra of the truncated ClpB variants indicate a significant loss in secondary structure, as compared to wt ClpB (Figure 5). The truncation-induced changes in secondary structure may involve the loss of structure within MD or, possibly, in other ClpB domains that may interact with MD.

To test the overall stability of ClpB and its truncated variants, we performed differential scanning calorimetry experiments (Figure 6). The DSC thermogram of wt ClpB shows two prominent unfolding transitions at 53 °C and 64 °C. The area of thermal transitions, which defines the unfolding enthalpy, is decreased in the truncated forms of ClpB: Δ417–455, Δ456–498, and Δ496–530. The ClpB variant Δ531–569 precipitated in the temperature range corresponding to the thermal transitions (not shown). Interestingly, the mid-point temperatures of DSC transitions for the ClpB variants shown in Figure 6 were not significantly affected by the deletions within MD. We conclude that although the deletions within MD affected significantly the enthalpy of unfolding of ClpB, the truncated variants Δ417–455, Δ456–498, and Δ496–530 retained significant amounts of the thermodynamically stable protein structure.

Figure 7 shows apparent distributions of the sedimentation coefficient ($g(s^*)$) for the full-length ClpB and the four truncated variants. ClpB forms oligomers under low-ionic strength conditions (27) and sediments in solution as a single molecular species with the sedimentation coefficient $s_{20,w}$ ~17.5 S (Figure 7A). In contrast, the variant Δ531–569 is monomeric (Figure 7E). The remaining three ClpB variants show a heterogeneity of the sedimenting species (Figure 7B, C, D). Whereas the variants Δ417–455, Δ456–498, and Δ496–530 show some self-association propensity in solution, only a fraction of the variant Δ496–530 fully associates into the wild type-like oligomers (Figure 7D). We conclude that the heptad-repeat deletions within MD strongly inhibit the self-association of ClpB.

Self-association of ClpB at physiological ionic strength can be also induced by binding of nucleotides (Figure 8A and (12;13;28)). As shown in Figure 8, ATP has only a small effect on the elution of Δ456–498 and Δ496–530 from a gel-filtration column and no effect on the elution of Δ417–455 and Δ531–569. We conclude that the defects in self-association of the truncated ClpB variants that are detected in the absence of nucleotides cannot be overcome by the binding of ATP.

As has been shown before, the oligomerization of ClpB is necessary for its ATPase activity because ATP binds very weakly to monomeric ClpB (13). Consistently, all four truncated variants of ClpB showed defects in the ability to hydrolyze ATP, as compared to wt ClpB (Table 1). The basal ATPase of the four truncated variants is lower than that of wt ClpB. Whereas the ATPase of wt ClpB is efficiently activated by casein or poly-lysine (Table 1 and (13;15;29)), only the ATPase of Δ496–530 responds weakly to casein and poly-lysine.

DISCUSSION

Studies aimed at understanding the mechanism of function of complex "protein machines" often focus on structural properties and biochemical roles of distinct domains within a protein in question. In the case of ClpB, such an approach produced a wealth of new information on the role of the N-terminal domain as well as subdomains within the AAA ATP-binding modules (13;15;17;24). The present study is the first attempt of a detailed analysis of the properties and role of the middle sequence region of ClpB, which appears to be uniquely related to the protein-disaggregating activity of ClpB. Whereas high-resolution structural information has been obtained for the N-terminal domain (30) and the D1 module in ClpB (31), no such information is available for the middle domain of ClpB or any other related Hsp100 protein.

We showed that the middle sequence region of ClpB (amino acids 410–570) folds into a stable domain with a structure dominated by α-helices (see Figure 2). In the crystal structure of ClpA (32), the two AAA modules are directly connected in a "head-to-tail" orientation. Thus, it is likely that in ClpB, the AAA modules are spatially separated by the inserted middle domain.

The α-helical structure of MD is consistent with heptad repeats and the predicted coiled-coil architecture (see Figure 1B). Genuine coiled-coils undergo efficient self-association into dimers and sometimes trimers or tetramers (19). Sedimentation equilibrium experiments showed, however, that MD is monomeric in solution at either low- or high-ionic strength (see Figure 3 and Results) in a broad protein-concentration range. Importantly, α-helical structure of oligomeric coiled-coils becomes unstable upon the dissociation of an oligomer (33;34). Since MD is stable and monomeric, we conclude that it does not behave as a *bona fide* coiled-coil. Instead, we propose that the apparent heptad repeats identified in MD stabilize intramolecular contacts between several α-helices within MD. A possibility that the MD heptad repeats interact with similar regions in other domains of ClpB is unlikely because no apparent heptad repeats have been found outside MD (20).

Studies on the truncated variants of ClpB with deletions of different segments of the heptad repeats show that MD plays an important structural role in ClpB. Each deletion apparently decreased the α-helical content of ClpB (see Figure 5), which is consistent with the heptad repeats stabilizing an α-helical bundle within MD (see above). Structural integrity of MD significantly contributes to the unfolding enthalpy of ClpB (see Figure 6). Most significantly, deletions within MD strongly inhibit the self-association of ClpB (see Figure 7).

It has been postulated that the biochemical activity of ClpB and other Clp ATPases depends on the ability of these proteins to form oligomers. Indeed, truncations and mutations in ClpB that inhibit its self-association also decrease the ATPase activity (12;13;17) presumably because monomeric ClpB binds nucleotides with a low affinity (13). The results of this study confirm the linkage in ClpB between protein oligomerization and the biochemical activity. Out of the four truncated variants of ClpB, only Δ456–498 and Δ496–530 form some oligomers in the absence of nucleotides (see Figure 7). Consistently, only Δ496–530 and, to a lower extent, Δ456–498 respond weakly to ATP in the gel filtration experiment (see Figure 8). Finally, the ATPase of all truncated ClpB variants is low, as compared to wt and only Δ496–530 shows activation of its ATPase in the presence of casein or poly-lysine (see Table 1).

In previous studies, truncated and mutated variants of ClpB with low ATPase activity also showed defects in the chaperone activity *in vitro* and *in vivo* (12;13;17;35). Consistently, we found low chaperone activity of ClpB with truncations within MD (see Figure 4). Taken together, our results show that the heptad repeats in MD stabilize a structure, possibly a multi-helix bundle within MD, that is essential for the self-association of ClpB and, as a consequence, for its ATPase and chaperone activity. A small protective effect of Δ417–455 *in vivo* (see Figure 4A) suggests that some elements of ClpB function (for example, binding of a substrate or a co-chaperone) may occur even in the absence of an efficient oligomerization and the ATPase activity.

What role could the middle domain play in stabilization of the structure of ClpB? Previous studies showed that ClpA, which does not contain MD, does not form ring-type oligomers in the absence of nucleotides or with ADP (32;36). In contrast, ClpB forms nucleotide-free and ADP-bound oligomers (12;28). The oligomeric architecture of ClpA (32) and other AAA^+ ATPases (37;38) implies that that two AAA modules form two distinct stacked rings within the AAA oligomer. In oligomeric ClpB, middle domains could form an additional ring sandwiched between the two AAA rings. Inter-subunit contacts within the ring of MDs could provide additional free energy for self-association of ClpB, as compared to ClpA. Since MD is monomeric in solution (see Figure 3), the proposed inter-subunit contacts most likely do not involve an inter-MD coiled-coil.

The crystal structure of ClpA suggested that the linkage between the two AAA modules (D1, D2) can be rotated to produce at least two distinct conformations (32). In ClpB the middle domain not only separates the AAA modules, but may also stabilize a ClpB-specific spatial orientation of D1 and D2, which is not found in ClpA.

References

1. Schirmer EC, Glover JR, Singer MA, Lindquist S. Trends Biochem Sci 1996;21:289–296. [PubMed: 8772382]
2. Neuwald AF, Aravind L, Spouge JL, Koonin EV. Genome Res 1999;9:27–43. [PubMed: 9927482]
3. Ogura T, Wilkinson AJ. Genes Cells 2001;6:575–597. [PubMed: 11473577]
4. Weber-Ban EU, Reid BG, Miranker AD, Horwich AL. Nature 1999;401:90–93. [PubMed: 10485712]
5. Singh SK, Grimaud R, Hoskins JR, Wickner S, Maurizi MR. Proc Natl Acad Sci U S A 2000;97:8898–8903. [PubMed: 10922052]
6. Burton RE, Siddiqui SM, Kim YI, Baker TA, Sauer RT. EMBO J 2001;20:3092–3100. [PubMed: 11406586]
7. Zolkiewski M. J Biol Chem 1999;274:28083–28086. [PubMed: 10497158]
8. Goloubinoff P, Mogk A, Zvi AP, Tomoyasu T, Bukau B. Proc Natl Acad Sci U S A 1999;96:13732–13737. [PubMed: 10570141]
9. Motohashi K, Watanabe Y, Yohda M, Yoshida M. Proc Natl Acad Sci U S A 1999;96:7184–7189. [PubMed: 10377389]
10. Glover JR, Lindquist S. Cell 1998;94:73–82. [PubMed: 9674429]
11. Queitsch C, Hong SW, Vierling E, Lindquist S. Plant Cell 2000;12:479–492. [PubMed: 10760238]
12. Barnett ME, Zolkiewski M. Biochemistry 2002;41:11277–11283. [PubMed: 12220194]
13. Barnett ME, Zolkiewska A, Zolkiewski M. J Biol Chem 2000;275:37565–37571. [PubMed: 10982797]
14. Lo JH, Baker TA, Sauer RT. Protein Sci 2001;10:551–559. [PubMed: 11344323]
15. Liu Z, Tek V, Akoev V, Zolkiewski M. J Mol Biol 2002;321:111–120. [PubMed: 12139937]
16. Beinker P, Schlee S, Groemping Y, Seidel R, Reinstein J. J Biol Chem 2002;277:47160–47166. [PubMed: 12351638]

17. Mogk A, Schlieker C, Strub C, Rist W, Weibezahn J, Bukau B. J Biol Chem 2003;278:17615–17624. [PubMed: 12624113]
18. Thomas JG, Baneyx F. Mol Microbiol 2000;36:1360–1370. [PubMed: 10931286]
19. Adamson JG, Zhou NE, Hodges RS. Curr Opin Biotechnol 1993;4:428–437. [PubMed: 7763973]
20. Celerin M, Gilpin AA, Schisler NJ, Ivanov AG, Miskiewicz E, Krol M, Laudenbach DE. J Bacteriol 1998;180:5173–5182. [PubMed: 9748452]
21. Skehel JJ, Wiley DC. Annu Rev Biochem 2000;69:531–569. [PubMed: 10966468]
22. Squires CL, Pedersen S, Ross BM, Squires C. J Bacteriol 1991;173:4254–4262. [PubMed: 2066329]
23. Churchward G, Belin D, Nagamine Y. Gene 1984;31:165–171. [PubMed: 6098521]
24. Tek V, Zolkiewski M. Protein Sci 2002;11:1192–1198. [PubMed: 11967375]
25. Shrake A, Fisher MT, McFarland PJ, Ginsburg A. Biochemistry 1989;28:6281–6294. [PubMed: 2571357]
26. Stafford WF III. Anal Biochem 1992;203:295–301. [PubMed: 1416025]
27. Kim KI, Cheong GW, Park SC, Ha JS, Woo KM, Choi SJ, Chung CH. J Mol Biol 2000;303:655–666. [PubMed: 11061966]
28. Zolkiewski M, Kessel M, Ginsburg A, Maurizi MR. Protein Sci 1999;8:1899–1903. [PubMed: 10493591]
29. Woo KM, Kim KI, Goldberg AL, Ha DB, Chung CH. J Biol Chem 1992;267:20429–20434. [PubMed: 1400361]
30. Li J, Sha B. Structure (Camb) 2003;11:323–328. [PubMed: 12623019]
31. Li J, Sha B. J Mol Biol 2002;318:1127–1137. [PubMed: 12054807]
32. Guo F, Maurizi MR, Esser L, Xia D. J Biol Chem 2002;277:46743–46752. [PubMed: 12205096]
33. Thompson KS, Vinson CR, Freire E. Biochemistry 1993;32:5491–5496. [PubMed: 8504069]
34. Zolkiewski M, Redowicz MJ, Korn ED, Hammer JA III, Ginsburg A. Biochemistry 1997;36:7876–7883. [PubMed: 9201932]
35. Watanabe YH, Motohashi K, Yoshida M. J Biol Chem 2002;277:5804–5809. [PubMed: 11741950]
36. Maurizi MR, Singh SK, Thompson MW, Kessel M, Ginsburg A. Biochemistry 1998;37:7778–7786. [PubMed: 9601038]
37. Rouiller I, DeLaBarre B, May AP, Weis WI, Brunger AT, Milligan RA, Wilson-Kubalek EM. Nat Struct Biol 2002;9:950–957. [PubMed: 12434150]
38. Zhang X, Shaw A, Bates PA, Newman RH, Gowen B, Orlova E, Gorman MA, Kondo H, Dokurno P, Lally J, Leonard G, Meyer H, van Heel M, Freemont PS. Mol Cell 2000;6:1473–1484. [PubMed: 11163219]

Abbreviations

MD
: middle domain of ClpB

CD
: circular dichroism

DSC
: differential scanning calorimetry

DTT
: dithiothreitol

A

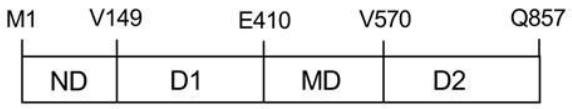

B

```
                    gabcdefgabcdefgabcd          gabcdefgabcdefgabcde          abcdefgabcdefgabcdefgabcde
wt ClpB    407 SKPEELDRLDRRIIQLKLEQQALMKESDEASKKRLDMLNEELSDKERQYSELEEEWKAEKASLSGTQTIKAELEQAKIAIEQARRVGDLARM 498
Δ417-455   407 SKPEELDRLD-----------------------------------SELEEEWKAEKASLSGTQTIKAELEQAKIAIEQARRVGDLARM 498
Δ456-498   407 SKPEELDRLDRRIIQLKLEQQALMKESDEASKKRLDMLNEELSDKERQK----------------------------------------
Δ496-530   407 SKPEELDRLDRRIIQLKLEQQALMKESDEASKKRLDMLNEELSDKERQYSELEEEWKAEKASLSGTQTIKAELEQAKIAIEQARRVGDL---
Δ531-569   407 SKPEELDRLDRRIIQLKLEQQALMKESDEASKKRLDMLNEELSDKERQYSELEEEWKAEKASLSGTQTIKAELEQAKIAIEQARRVGDLARM 498

                      gabcdefgabcde                              defgabcdefgabcdefga
wt ClpB    499 SELQYGKIPELEKQLEAATQLEGKTMRLLRNKVTDAEIAEVLARWTGIPVSRMMESEREKLLRMEQELHHRVIG 572
Δ417-455   499 SELQYGKIPELEKQLEAATQLEGKTMRLLRNKVTDAEIAEVLARWTGIPVSRMMESEREKLLRMEQELHHRVIG 572
Δ456-498   499 SELQYGKIPELEKQLEAATQLEGKTMRLLRNKVTDAEIAEVLARWTGIPVSRMMESEREKLLRMEQELHHRVIG 572
Δ496-530       --------------------------------VTDAEIAEVLARWTGIPVSRMMESEREKLLRMEQELHHRVIG 572
Δ531-569   499 SELQYGKIPELEKQLEAATQLEGKTMRLLRNK-----------------------------------------VIG 572
```

Figure 1.

(A) Postulated domain structure of ClpB. The diagram shows two AAA ATP-binding modules (D1, D2), the N-terminal domain (ND), and the middle domain (MD). (B) The amino-acid sequence of the middle domain of ClpB from *Escherichia coli* (wt ClpB) and four ClpB variants containing deletions within MD produced in this study. The sequence regions showing apparent coiled-coil heptad repeats (*a* through *g*) are indicated.

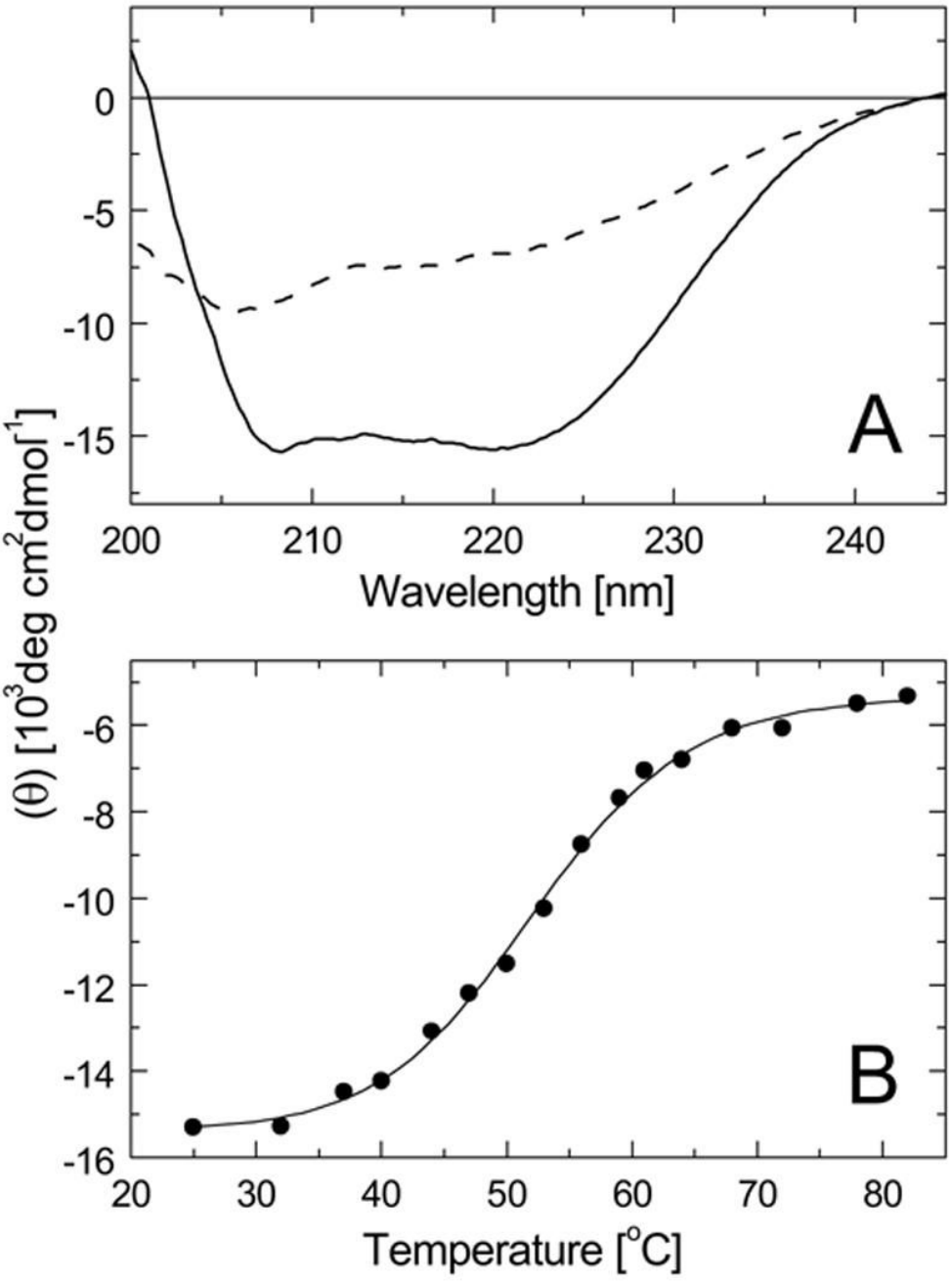

Figure 2.

Circular dichroism and thermal stability of the middle domain of ClpB. (A) Far-UV CD spectra of the isolated middle domain of ClpB at 25 °C (solid line) and 82 °C (broken line). The protein concentration was 1 mg/ml in 50 mM Tris-HCl at pH 7.5, 0.2 M KCl, 20 mM $MgCl_2$, 10% glycerol, 1 mM EDTA. The CD signal was expressed as mean molar residue ellipticity. (B) Temperature-induced changes in the CD signal at 222 nm for the middle domain of ClpB. Solid line shows the fit of a two-state unfolding model.

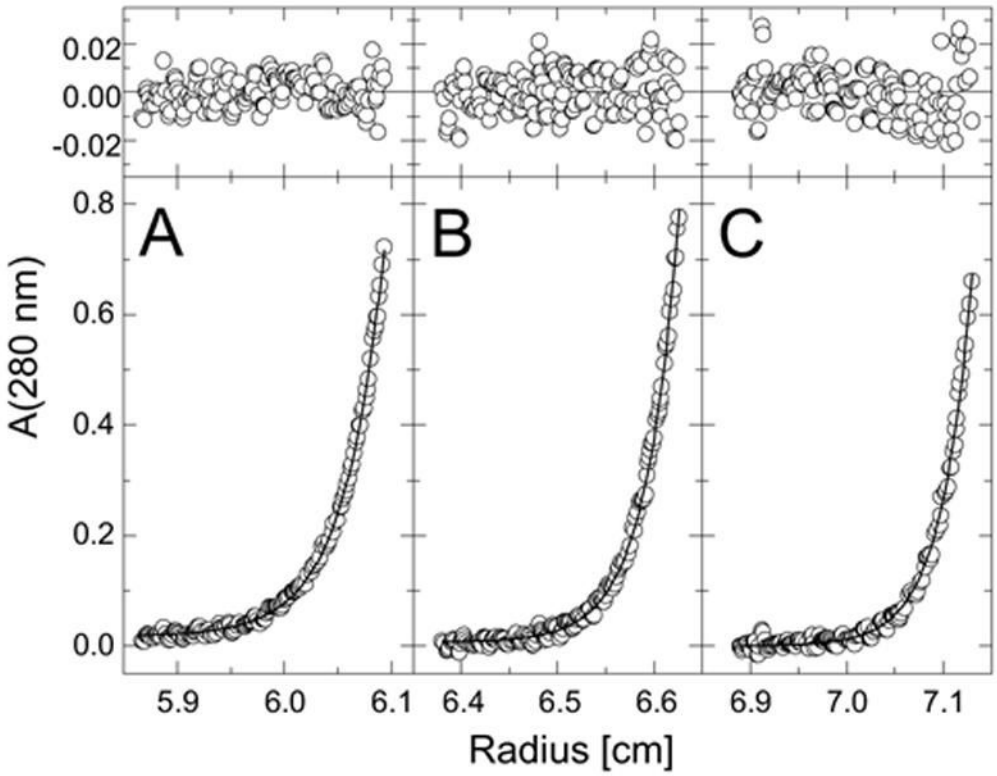

Figure 3.

Sedimentation equilibrium analysis of the isolated middle domain of ClpB. Ultracentrifugation was performed at 40,000 rpm and 4 °C. The protein was loaded in the centrifuge cell at 2 mg/ml (A), 1 mg/ml (B), and 0.5 mg/ml (C) in Hepes-KOH (pH 7.5), 20 mM $MgCl_2$, 1 mM EDTA. Protein concentration gradients at equilibrium are shown in the lower panels (circles) along with the fits corresponding to a single molecular component of the 20,940 molecular weight (solid lines). The upper panels show residuals of the fits (A_{exp}-A_{fit}). Three data sets shown in panels A, B, C were simultaneously included in the molecular weight determination.

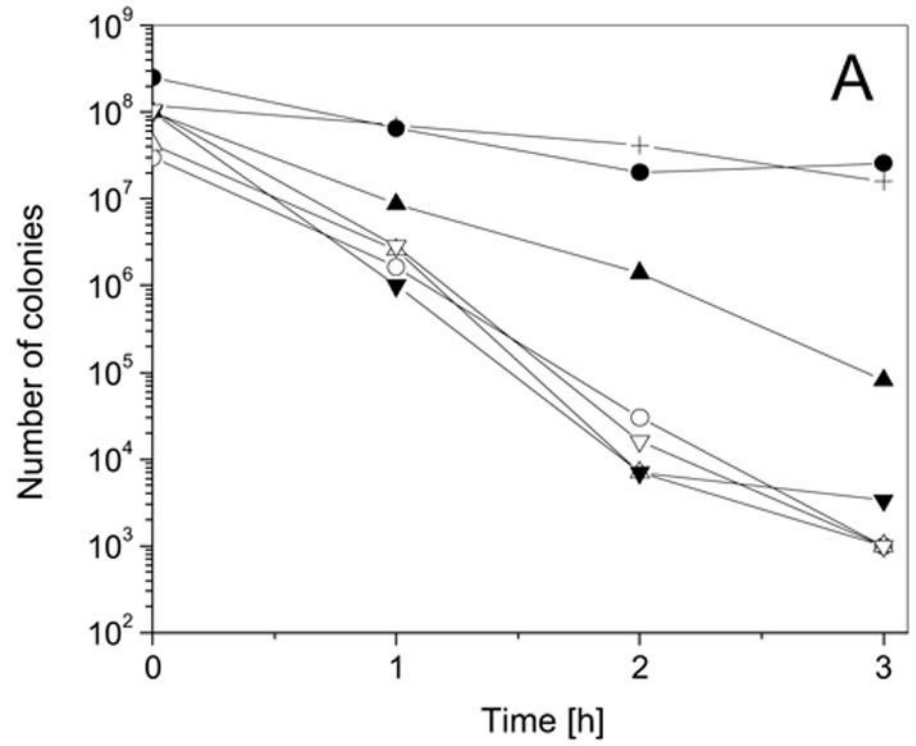

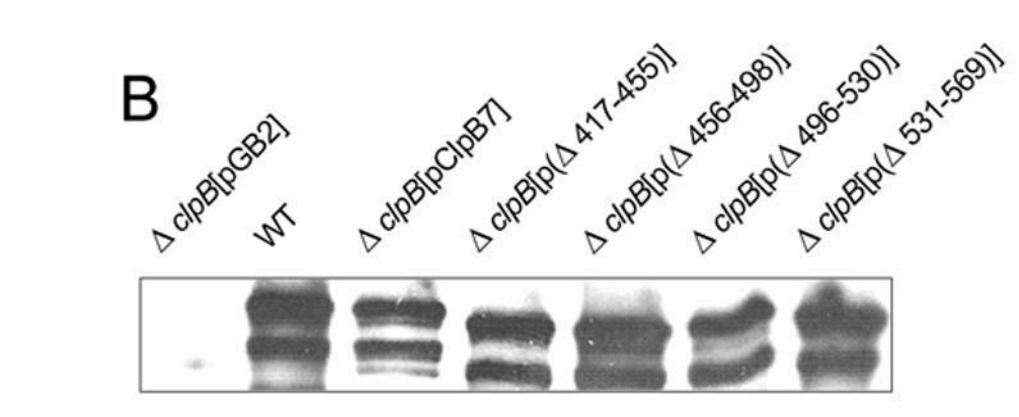

Figure 4.

(A) *In vivo* activity of ClpB and its truncated variants. *E. coli* cells were grown under heat-shock conditions at 50 °C. At the indicated time, cells were removed from the culture, serially diluted, and spotted on LB agar plates. Cell survival was measured as the number of colonies after an overnight incubation at 37 °C. The data are shown for wild type MC4100 *E. coli* (filled circles), ClpB-null MC4100 Δ*clpB*[pGB2] (open circles), MC4100 Δ*clpB*[pClpB7] (crosses), MC4100 Δ*clpB*[p(Δ417–455)] (filled triangles), MC4100Δ*clpB*[p(Δ456–498)] (open triangles), MC4100Δ*clpB*[p(Δ496–530)] (filled inverted triangles), and MC4100Δ*clpB*[p(Δ531–569)] (open inverted triangles). Averages from a series of three experiments are shown. (B) Production of ClpB in the bacterial strains under heat-shock. After 2 h of heat-shock,

aliquots of bacterial cultures were analyzed by SDS-PAGE followed by Western blotting using anti-ClpB antibodies. Two immunoreactive bands correspond to the full-length and the naturally occurring N-terminally truncated ClpB.

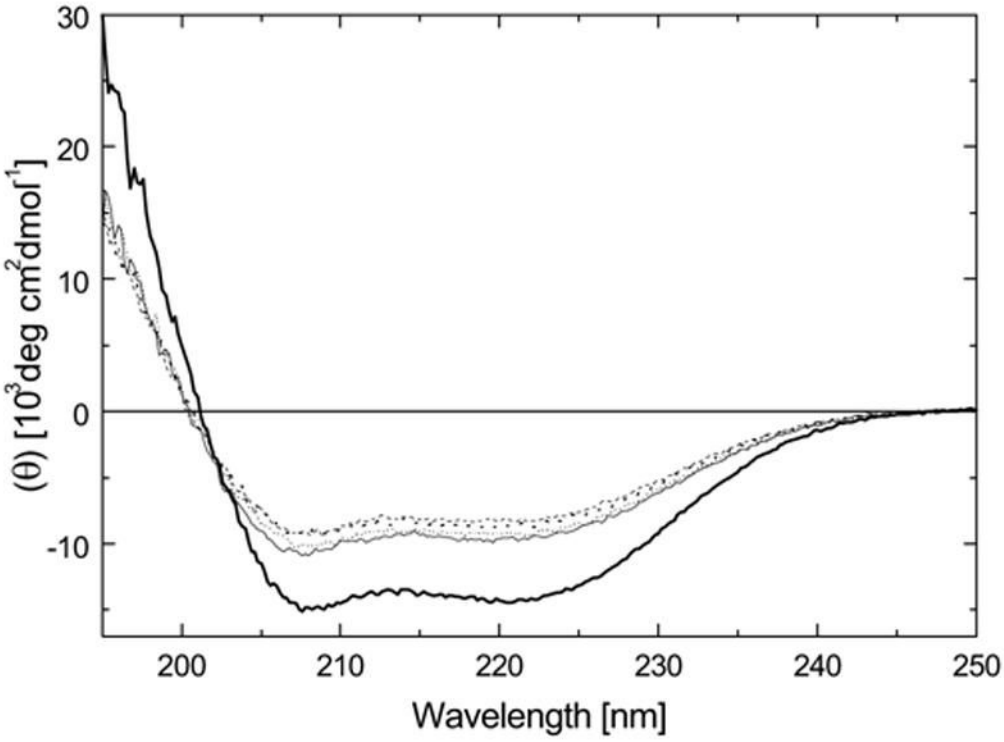

Figure 5.

Far-UV circular dichroism spectra of ClpB and its truncated variants. The CD signal is expressed as mean molar residue ellipticity (θ) and shown for wild type ClpB (thick solid line), Δ417–455 (thin solid line), Δ456–498 (thin broken line), Δ496–530 (dotted line), and Δ531–569 (thick dotted line). The protein concentration was 1 mg/ml in 50 mM Tris-HCl (pH 7.5), 0.2 M KCl, 20 mM $MgCl_2$, 10% glycerol, 1 mM EDTA, 1 mM DTT.

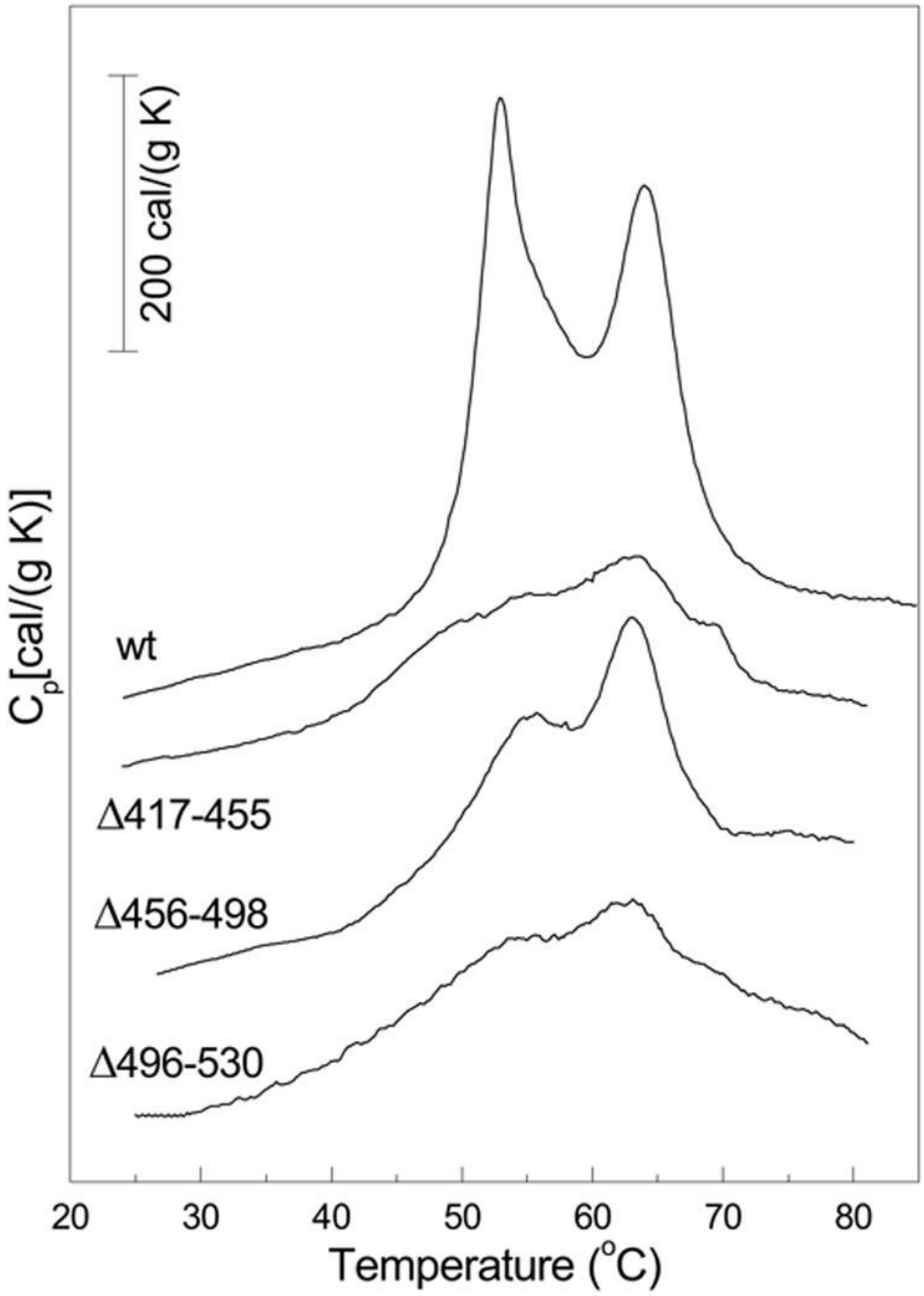

Figure 6.

Differential scanning calorimetry of ClpB and its truncated variants. DSC thermograms were obtained at the 1 K/min scan-rate for 0.7 mg/mL protein. Baselines measured with the dialyzate buffer (50 mM Hepes-KOH, pH 7.5) without the proteins were subtracted from the protein scans. The DSC data were normalized for protein concentration and variable offsets were applied to the data sets for clarity of presentation.

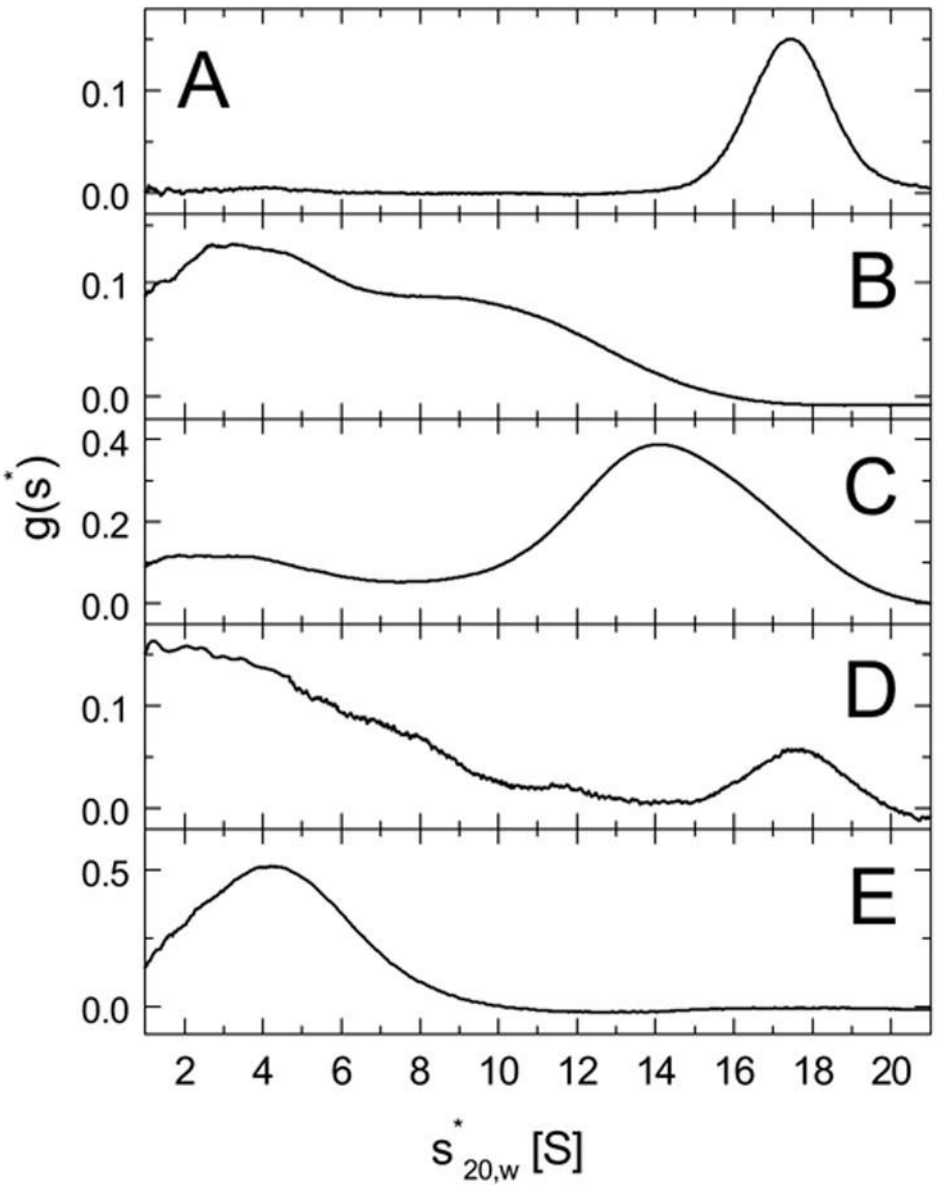

Figure 7.

Sedimentation velocity analysis of the truncated variants of ClpB. Ultracentrifugation was performed at 40,000 rpm and 20 °C. The protein concentration was ~1.5 mg/mL in 50 mM Hepes-KOH (pH 7.5), 20 mM $MgCl_2$, 1 mM EDTA and 1 mM β -mercaptoethanol. Protein concentration profiles in the centrifuge cell were measured using the interference detection system. Apparent sedimentation distributions g(*s**) vs. $s^*_{20,w}$ in Svedbergs (S) are shown for the full-length ClpB (A), Δ417–455 (B), Δ456–498 (C), Δ496–530 (D), and Δ531–569 (E).

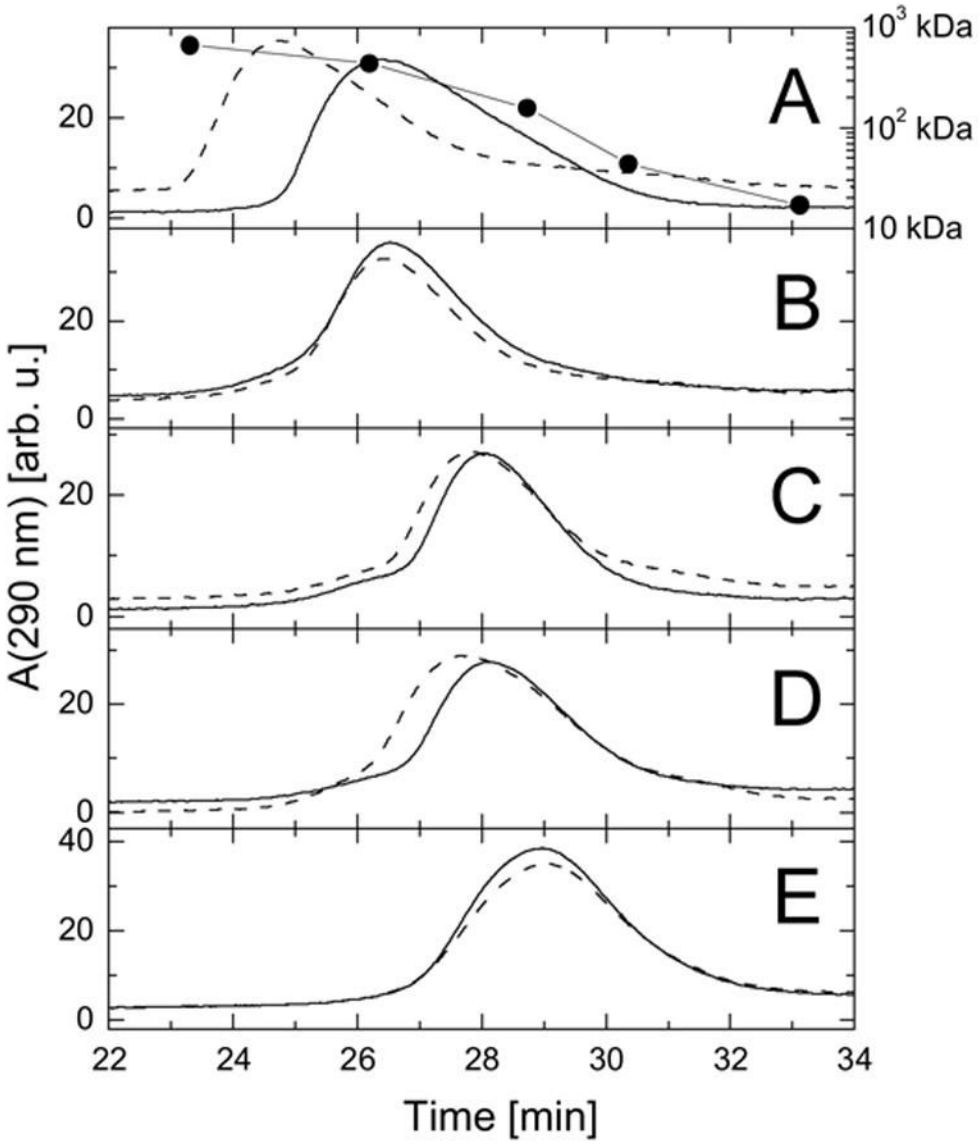

Figure 8.

Gel-filtration analysis of ClpB and its truncated variants. Aliquots of the full-length ClpB (A), Δ417–455 (B), Δ456–498 (C), Δ496–530 (D), and Δ531–569 (E) were injected onto a Superose 6 column equilibrated with 50 mM Tris-HCl, pH 7.5, 0.2 M KCl, 20 mM $MgCl_2$, 1 mM EDTA, and 1 mM DTT. Protein elution profiles were obtained at a flow-rate of 0.05 ml/min in the absence of nucleotides (solid lines) or with 2 mM ATP in the running buffer (broken lines). Circles in panel A correspond to the elution times of thyroglobulin (M_r, 670,000), apoferritin (M_r, 443,000), γ-globulin (M_r, 158,000), ovalbumin (M_r, 44,000), and myoglobin (M_r, 17,000).

Table 1

ATPase activity of ClpB and its truncated variants[a]

Protein	ATPase activity [pmol/(min μg)]		
	basal	casein-activated	pLys-activated
wt ClpB	110 ± 10	490 ± 30	1590 ± 330
Δ417–455	3.05 ± 0.40	13.0 ± 1.2	11.6 ± 1.5
Δ456–498	2.03 ± 0.28	20.7 ± 1.2	15.4 ± 2.9
Δ496–530	47.0 ± 2.3	146 ± 34	163 ± 37
Δ531–569	32.8 ± 3.3	48.0 ± 4.1	66.0 ± 2.7

[a] Initial rates of ATP hydrolysis (average ± SD from 6 determinations) are reported for ClpB in the absence of other proteins (basal activity), with 0.1 mg/mL κ-casein (casein activated), or with 0.01 mg/mL poly-L-lysine (pLys-activated).